

University of Wisconsin - Madison

MADPH-96-939

UCD-96-12

April 1996

Particle Physics Opportunities at $\mu^+\mu^-$ Colliders*

V. Barger^a, M.S. Berger^b, J.F. Gunion^c, T. Han^c

^aPhysics Department, University of Wisconsin, Madison, WI 53706, USA

^bPhysics Department, Indiana University, Bloomington, IN 47405, USA

^cPhysics Department, University of California, Davis, CA 95616, USA

We discuss the capabilities of future muon colliders to resolve important particle physics questions. A collider with c.m. energy $\sqrt{s} = 100$ to 500 GeV offers the unique opportunity to produce Higgs bosons in the s -channel and thereby measure the Higgs masses, total widths and several partial widths to high precision. At this same machine, $t\bar{t}$ and W^+W^- threshold studies would yield superior precision in the determination of m_t and m_W . A multi-TeV $\mu^+\mu^-$ collider would open up the realm of physics above the 1 TeV scale, allowing, for example, copious production of supersymmetric particles up to the highest anticipated masses or a detailed study of the strongly-interacting scenario of electroweak symmetry breaking.

1. INTRODUCTION

There is increasing interest recently in the possible construction of a $\mu^+\mu^-$ collider[1,2,3,4]. The expectation is that a muon collider with energy and integrated luminosity comparable to or superior to those attainable at e^+e^- colliders can be achieved[5,6,7]. An initial survey of the physics potential of muon colliders has been carried out[8]. In this report we summarize some of the progress on the physics issues that has been made in the last year; a more comprehensive report is in preparation[9].

One of the primary arguments for an e^+e^- collider is the complementarity with physics studies at the LHC. The physics potential of a muon collider is comparable to that of an electron collider with the same energy and luminosity. How-

ever, electron colliders are at a technologically more advanced stage and will likely be built before muon colliders. Hence a very relevant issue is what can be done at a muon collider that cannot be done at an electron collider.

The advantages of a muon collider can be summarized briefly as follows:

- The muon is significantly heavier than the electron, and therefore couplings to Higgs bosons are enhanced making possible their study in the s -channel production process.
- The limitation on luminosity from beam-beam interactions that arises at an e^+e^- collider is not relevant for muon beam energies below about 100 TeV; very small/flat beams are unnecessary. Instead, large luminosity is achieved for $\sim 3\mu\text{m}$ size beams by storing multiple bunches in the final storage ring and having a large number of turns of storage per cycle. Radiative losses in the storage ring are small due to the large muon mass. Thus, extending the energy reach of these colliders well beyond the 1 TeV range is possible.
- The muon collider can be designed to have finer energy resolution than an e^+e^- machine.
- At a muon collider, $\mu^+\mu^+$ and $\mu^-\mu^-$ collisions are likely to be as easily achieved as $\mu^+\mu^-$ collisions.

There are two slight drawbacks of a muon collider. The first is that substantial polarization of the beams can probably not be achieved without sacrificing luminosity. The second drawback

*Based on talks given at the *Symposium on Physics Potential and Development of $\mu^+\mu^-$ Colliders*, San Francisco, California, December 13–15, 1995.

is that the $\gamma\gamma$ and $\mu\gamma$ options are probably not feasible. At future linear e^+e^- colliders, the possibility exists to backscatter laser photons off the electron and/or positron beams. The resulting back-scattered photons are highly collimated and could serve as a photon beam, thus converting the e^+e^- collider to a $e\gamma$ or $\gamma\gamma$ collider. The collisions from the back-scattered photons have center-of-mass energies that range up almost to that of the parent e^+e^- collider. Including this option at a $\mu^+\mu^-$ collider is problematic from kinematic considerations. The highest photon energy ω attainable from a lepton with energy E is

$$\frac{\omega_{\max}}{E} = \frac{x}{x+1}, \quad (1)$$

where

$$x = \frac{4E\omega_0}{m_\mu^2 c^4}. \quad (2)$$

For a muon collider $x \ll 1$ unless a laser photon energy ω_0 of the order of keV is possible, which seems unlikely.

A proposed schematic design for a muon collider is shown in Fig. 1. Protons produce π 's in a fixed target which subsequently decay giving μ 's. The muons must be collected, cooled and subsequently accelerated to high energies. Since the muon is so much heavier than the electron, synchrotron radiation is much less so that circular storage rings are feasible even at TeV energies.

The monochromaticity of the beams will prove critically important for some of the physics that can be done at a $\mu^+\mu^-$ collider. The energy profile of the beam is expected to be roughly Gaussian in shape, and the rms deviation R is expected to naturally lie in the range $R = 0.04\%$ to 0.08% [10]. Additional cooling could further sharpen the beam energy resolution to $R = 0.01\%$.

Two possible $\mu^+\mu^-$ machines have been discussed as design targets and are being actively studied [2,3,4]:

- (i) A first muon collider (FMC) with low c. m. energy (\sqrt{s}) between 100 and 500 GeV and $\mathcal{L} \sim 2 \times 10^{33} \text{ cm}^{-2} \text{ s}^{-1}$ delivering an annual integrated integrated luminosity $L \sim 20 \text{ fb}^{-1}$.
- (ii) A next muon collider (NMC) with high $\sqrt{s} \gtrsim 4 \text{ TeV}$ and $\mathcal{L} \sim 10^{35} \text{ cm}^{-2} \text{ s}^{-1}$ giving $L \sim 1000 \text{ fb}^{-1}$ yearly.

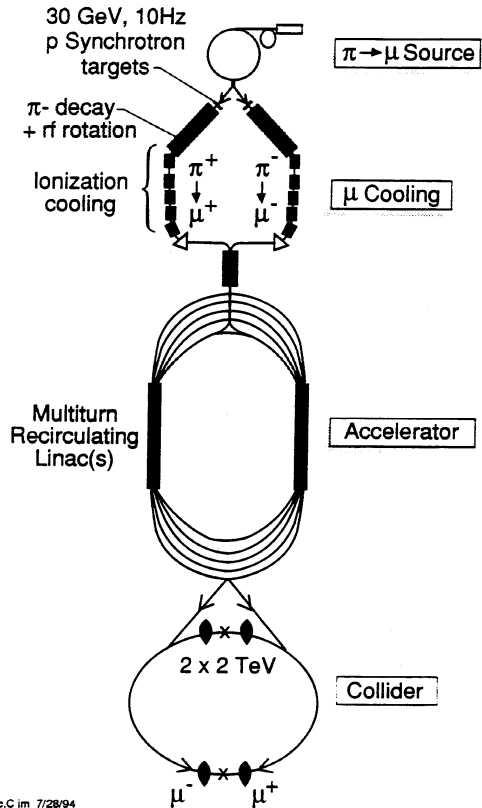


Figure 1: A possible design for a muon collider, from Ref. [2].

2. s -CHANNEL HIGGS PHYSICS

The simplest Higgs sector is that of the Standard Model (SM) with one Higgs boson. However, the naturalness and hierarchy problems that arise in the SM and the failure of grand unification of couplings in the SM suggest that a single Higgs boson is probably not the whole story of electroweak symmetry breaking. Therefore, it is crucially important to understand and delineate experimentally various alternative possibilities.

Supersymmetry is an especially attractive candidate theory in that it solves the naturalness and hierarchy problems (for a sufficiently low scale of supersymmetry breaking) and in that scalar bosons, including Higgs bosons, are on the same footing as fermions as part of the particle spec-

trum. The minimal supersymmetric model (MSSM) is the simplest SUSY extension of the SM. In the MSSM, every SM particle has a superpartner. In addition, the minimal model contains exactly two Higgs doublets. At least two Higgs doublet fields are required in order that both up and down type quarks be given masses without breaking supersymmetry (and also to avoid anomalies in the theory). Exactly two doublets allows unification of the SU(3), SU(2) and U(1) coupling constants. (Extra Higgs singlet fields are allowed by unification, but are presumed absent in the MSSM.) For two Higgs doublets and no Higgs singlets, the Higgs spectrum comprises 5 physical Higgs bosons

$$h^0, H^0, A^0, H^+, H^- . \quad (3)$$

The quartic couplings in the MSSM Higgs potential are related to the electroweak gauge couplings g and g' and the tree-level Higgs mass formulas imply an upper bound on the mass of the lightest Higgs boson, $m_h \leq M_Z$. At one loop, the radiative correction to the mass of the lightest Higgs state depends on the top and stop masses

$$\delta m_{h^0}^2 \simeq \frac{3g^2}{8\pi^2 m_W^2} m_t^4 \ln \left(\frac{m_{\tilde{t}_1} m_{\tilde{t}_2}}{m_t^2} \right) . \quad (4)$$

Two-loop corrections are also significant. The resulting ironclad upper bounds on the possible mass of the lightest Higgs boson are

$$m_{h^0} \lesssim 130 \text{ GeV} \quad \text{MSSM}, \quad (5)$$

$$m_{h^0} \lesssim 150 \text{ GeV} \quad \text{any SUSY GUT}, \quad (6)$$

$$m_{h^0} \lesssim 200 \text{ GeV} \quad \text{any model with} \quad (7)$$

GUT and desert.

In the largest part of parameter space, e.g. $m_{A^0} > 150 \text{ GeV}$ in the MSSM, the lightest Higgs boson has fairly SM-like couplings.

The first discovery of a light Higgs boson is likely to occur at the LHC which might be operating for several years before a next-generation lepton collider is built. Following its discovery, interest will focus on measurements of its mass, total width, and partial widths. A first question then is what could be accomplished at the Large Hadron Collider (LHC) or the Next Linear Collider (NLC) in this regard.

At the LHC, a SM-like Higgs can be discovered either through gluon fusion, followed by $\gamma\gamma$ or 4ℓ decay,

$$gg \rightarrow h \rightarrow \gamma\gamma , \quad (8)$$

$$gg \rightarrow h \rightarrow ZZ^* \rightarrow 4\ell , \quad (9)$$

or through associated production

$$gg \rightarrow t\bar{t}h \quad \begin{array}{l} \searrow \\ \downarrow \\ \swarrow \end{array} \gamma\gamma , \quad (10)$$

$$q\bar{q} \rightarrow Wh \quad \begin{array}{l} \searrow \\ \downarrow \\ \swarrow \end{array} \gamma\gamma . \quad (11)$$

The LHC collaborations report that the Higgs boson is detectable in the mass range $50 \lesssim m_h \lesssim 150 \text{ GeV}$ via its $\gamma\gamma$ decay mode. The mass resolution is expected to be $\lesssim 1\%$. At the NLC the Higgs boson is produced in the Bjorken process

$$e^+e^- \rightarrow Z^* \rightarrow Zh \quad (12)$$

and the h can be studied through its dominant $b\bar{b}$ decay. At the NLC (which may be available prior to a $\mu^+\mu^-$ collider) the mass resolution is strongly dependent on the detector performance and signal statistics:

$$\Delta m_h \simeq R_{\text{event}}(\text{GeV})/\sqrt{N} , \quad (13)$$

where R_{event} is the single event resolution and N is the number of signal events. The single event resolution is about 4 GeV for an SLD-type detector[11], but improved performance as typified by the ‘‘super’’-LC detector would make this resolution about 0.3 GeV[12,13]. The uncertainty in the Higgs boson mass for various integrated luminosities is shown in Fig. 2. For a Higgs boson with Standard Model couplings this gives a Higgs mass determination of

$$\Delta m_{h_{SM}} \simeq 400 \text{ MeV} \left(\frac{10 \text{ fb}^{-1}}{L} \right)^{1/2} , \quad (14)$$

for the SLD-type detector.

Precision measurements of the Higgs total width and partial widths will be necessary to distinguish between the predictions of the SM Higgs boson h_{SM} and the MSSM Higgs boson h^0 . Can the total and partial widths be measured at other machines? This is a complicated question since each

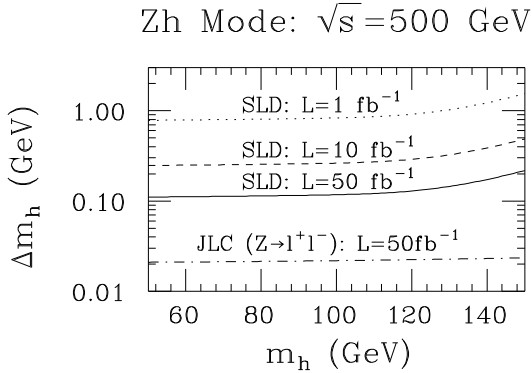


Figure 2: The uncertainty $\pm\Delta m_h$ in the determination of m_h for a SM-like Higgs boson using Zh production and a ± 4 GeV (“SLD”) or ± 0.3 GeV (“JLC”) single event mass resolution for m_h .

machine contributes different pieces to the puzzle. The bottom line[14] is that the LHC, NLC, and $\gamma\gamma$ colliders each measure interesting couplings and/or branching ratios, but their ability to detect deviations due to the differences between the h^0 and h_{SM} is limited to $m_{A^0} \lesssim 300$ GeV. Further, a model-independent study of all couplings and widths requires all three machines with consequent error propagation problems.

The s -channel process $\mu^+\mu^- \rightarrow b\bar{b}$ shown in Fig. 3 is uniquely suited to several critical precision Higgs boson measurements [15,16]. Detecting and studying the Higgs boson in the s -channel would require that the machine energy be adjusted to correspond to the Higgs mass. Since the storage ring is only a modest fraction of the overall muon collider cost[17], a special-purpose ring could be built to optimize the luminosity near the Higgs peak.

The s -channel Higgs phenomenology is set by the \sqrt{s} rms Gaussian spread denoted by $\sigma_{\sqrt{s}}$. A convenient formula for $\sigma_{\sqrt{s}}$ is

$$\sigma_{\sqrt{s}} = (7 \text{ MeV}) \left(\frac{R}{0.01\%} \right) \left(\frac{\sqrt{s}}{100 \text{ GeV}} \right). \quad (15)$$

A crucial consideration is how this natural spread in the muon collider beam energy compares to the width of the Higgs bosons, given in Fig. 4. In particular, a direct scan measurement of the Higgs width requires a beam spread comparable to the width. The narrowest Higgs boson widths

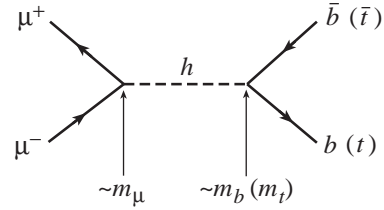


Figure 3: Feynman diagram for s -channel production of a Higgs boson.

are those of a light SM Higgs boson with mass $\lesssim 100$ GeV. In the limit where the heavier MSSM Higgs bosons become very massive, the lightest supersymmetric Higgs typically has a mass of order 100 GeV and has couplings that are sufficiently SM-like that its width approaches that of a light h_{SM} of the same mass. In either case, the discriminating power of a muon collider with a very sharp energy resolution would be essential for a direct width measurement.

A quantitative examination of Fig. 4 shows that for typical muon beam resolution ($R = 0.06\%$)

$$\sigma_{\sqrt{s}} \gg \Gamma_{h_{SM}}, \text{ for } m_{h_{SM}} \sim 100 \text{ GeV}, \quad (16)$$

$$\sigma_{\sqrt{s}} \sim \Gamma_{h^0}, \text{ for } m_{h^0} \text{ not near } m_{h^0}^{\text{max}}, \quad (17)$$

$$\sigma_{\sqrt{s}} \lesssim \Gamma_{H^0}, \Gamma_{A^0}, \text{ at moderate } \tan\beta, \quad (18)$$

for $m_{H^0, A^0} \sim 400$ GeV,

$$\ll \Gamma_{H^0}, \Gamma_{A^0}, \text{ at large } \tan\beta, \quad (19)$$

for $m_{H^0, A^0} \sim 400$ GeV.

To be sensitive to the $\Gamma_{h_{SM}}$ case, a resolution $R \sim 0.01\%$ is mandatory. This is an important conclusion given that such a small resolution requires early consideration in the machine design.

The s -channel Higgs resonance cross section is

$$\sigma_h = \frac{4\pi\Gamma(h \rightarrow \mu\mu)\Gamma(h \rightarrow X)}{(\hat{s} - m_h^2)^2 + m_h^2[\Gamma_h^{\text{tot}}]^2}, \quad (20)$$

where $\hat{s} = (p_{\mu^+} + p_{\mu^-})^2$ is the c. m. energy squared of the event, X denotes a final state and Γ_h^{tot} is the total width. The effective cross section is obtained by convoluting this resonance form with the Gaussian distribution of width $\sigma_{\sqrt{s}}$ centered at \sqrt{s} . When the Higgs width is much smaller than $\sigma_{\sqrt{s}}$, the effective signal cross section result

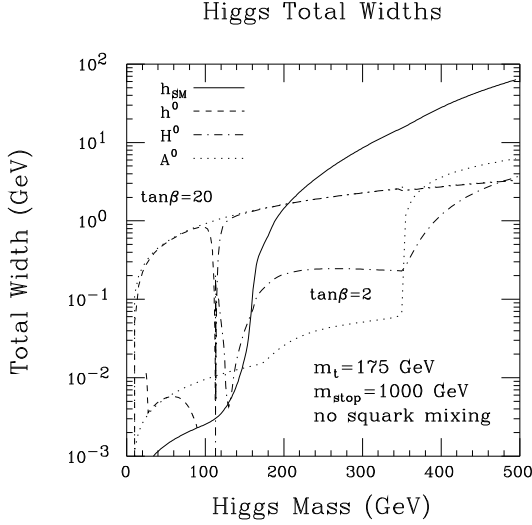


Figure 4: Total width versus mass of the SM and MSSM Higgs bosons for $m_t = 175$ GeV. In the case of the MSSM, we have plotted results for $\tan\beta = 2$ and 20 , taking $m_{\tilde{t}} = 1$ TeV and including two-loop corrections following Refs. [18,19] neglecting squark mixing; SUSY decay channels are assumed to be absent.

for $\sqrt{s} = m_h$, denoted by $\bar{\sigma}_h$, is

$$\bar{\sigma}_h = \frac{2\pi^2\Gamma(h \rightarrow \mu\mu)BF(h \rightarrow X)}{m_h^2} \times \frac{1}{\sigma_{\sqrt{s}}\sqrt{2\pi}}. \quad (21)$$

In the other extreme, where the Higgs width is much broader than $\sigma_{\sqrt{s}}$, at $\sqrt{s} = m_h$ we obtain

$$\bar{\sigma}_h = \frac{4\pi BF(h \rightarrow \mu\mu)BF(h \rightarrow X)}{m_h^2}. \quad (22)$$

Figure 5 illustrates the result of this convolution as a function of \sqrt{s} for \sqrt{s} near m_h in the three situations: $\Gamma_h^{\text{tot}} \ll \sigma_{\sqrt{s}}$, $\Gamma_h^{\text{tot}} \sim \sigma_{\sqrt{s}}$ and $\Gamma_h^{\text{tot}} \gg \sigma_{\sqrt{s}}$. We observe that small R greatly enhances the peak cross section for $\sqrt{s} = m_h$ when $\Gamma_h^{\text{tot}} \ll \sigma_{\sqrt{s}}$, as well as providing an opportunity to directly measure Γ_h^{tot} .

As an illustration, suppose $m_h \sim 110$ GeV and h is detected in $e^+e^- \rightarrow Zh$ or $\mu^+\mu^- \rightarrow Zh$ with mass uncertainty $\delta m_h \sim \pm 0.8$ GeV (obtained with luminosity $L \sim 1 \text{ fb}^{-1}$). For a standard model Higgs of this mass, the width is about 3.1 MeV. How many scan points and how much

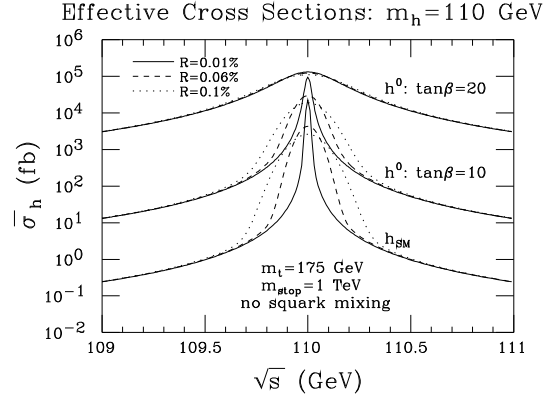


Figure 5: The effective cross section, $\bar{\sigma}_h$, obtained after convoluting σ_h with the Gaussian distributions for $R = 0.01\%$, $R = 0.06\%$, and $R = 0.1\%$, is plotted as a function of \sqrt{s} taking $m_h = 110$ GeV.

luminosity are required to zero in on $m_{h_{SM}}$ to within one rms spread $\sigma_{\sqrt{s}}$? For $R = 0.01\%$ ($R = 0.06\%$), $\sigma_{\sqrt{s}} \sim 7.7$ MeV (~ 45 MeV) and the number of scan points required to cover the 1.6 GeV mass zone at intervals of $\sigma_{\sqrt{s}}$ will be 230 (34), respectively. The luminosity required to observe (or exclude) the Higgs at each point is $L \gtrsim 0.01 \text{ fb}^{-1}$ ($L \gtrsim 0.3 \text{ fb}^{-1}$) for $R = 0.01\%$ ($R = 0.06\%$). Thus, the total luminosity required to zero in on the Higgs will be $\sim 2.3 \text{ fb}^{-1}$ ($\sim 10.2 \text{ fb}^{-1}$) in the two cases.

More generally, the L required at each scan point decreases as (roughly) $R^{1.7}$, whereas the number of scan points only grows like $1/R$, implying that the total L required for the scan decreases as $\sim R^{0.7}$. Thus, the $\mu^+\mu^-$ collider should be constructed with the smallest possible R value with the proviso that the number of \sqrt{s} settings can be correspondingly increased for the required scan. It must be possible to quickly and precisely adjust the energy of the $\mu^+\mu^-$ collider to do the scan.

To measure the width of a SM-like Higgs boson, one would first determine m_h to within $d\sigma_{\sqrt{s}}$ with $d \lesssim 0.3$ and then measure the cross section accurately at the wings of the excitation peak, see Fig. 5. The two independent measurements of $\sigma_{\text{wings}}/\sigma_{\text{peak}}$ give improved precision for the Higgs mass and determine the Higgs width. It is advantageous to put more luminosity on the

wings than the peak. Thus, to extract the total width we propose the following procedure[16]. First, conduct a rough scan to determine m_h to a precision $\sigma_{\sqrt{s}}d$, with $d \lesssim 0.3$. Then perform three measurements. At $\sqrt{s}_1 = m_h + \sigma_{\sqrt{s}}d$ expend a luminosity L_1 and measure the total rate $N_1 = S_1 + B_1$. Then perform measurements at

$$\sqrt{s}_2 = \sqrt{s}_1 - n_{\sigma_{\sqrt{s}}}\sigma_{\sqrt{s}} \quad (23)$$

and one at

$$\sqrt{s}_3 = \sqrt{s}_1 + n_{\sigma_{\sqrt{s}}}\sigma_{\sqrt{s}} \quad (24)$$

yielding $N_2 = S_2 + B_2$ and $N_3 = S_3 + B_3$ events, respectively, with luminosities of $L_2 = \rho_2 L_1$ and $L_3 = \rho_3 L_1$. The backgrounds can be determined from measurements farther from the resonance or from theoretical predictions. Next evaluate the ratios $r_2 = (S_2/\rho_2)/S_1$ and $r_3 = (S_3/\rho_3)/S_1$, for which the partial decay rates in the numerator in Eq. (20) cancel out. Since the excitation curve has a specific shape given by convoluting the denominator in Eq. (20) with the Gaussian distribution, these measured ratios determine the mass and total width of the Higgs boson. We find that the choices $n_{\sigma_{\sqrt{s}}} \simeq 2$ and $\rho_2 = \rho_3 \simeq 2.5$ are roughly optimal when $\sigma_{\sqrt{s}} \gtrsim \Gamma_h^{\text{tot}}$. For these choices and $R = 0.01\%$, a total luminosity $L = L_1 + L_2 + L_3$ of 2 fb^{-1} (200 fb^{-1}) would be required to measure Γ_h^{tot} with an accuracy of $\pm 30\%$ for $m_h = 110 \text{ GeV}$ ($m_h = m_Z$). An accuracy of $\pm 10\%$ for Γ_h^{tot} could be achieved for reasonable luminosities provided m_h is not near m_Z .

It must be stressed that the ability to precisely determine the energy of the machine when the three measurements are taken is crucial for the success of the three-point technique. A mis-determination of the *spacing* of the measurements in Eqs. (23) and (24) by just 3% would result in an error in $\Gamma_{h_{SM}}^{\text{tot}}$ of 30%. This does not present a problem provided some polarization of the beam can be achieved so that the precession of the spin of the muon as it circulates in the final storage ring can be measured. Given this and the rotation rate, the energy can be determined to the nearly 1 part in a million accuracy required. This energy calibration capability must be incorporated in the machine design from the beginning.

The other quantity that can be measured with great precision at a $\mu^+\mu^-$ collider for a SM-like Higgs with $m_h \lesssim 130 \text{ GeV}$ is $G(b\bar{b}) \equiv \Gamma(h \rightarrow \mu^+\mu^-)BF(h \rightarrow b\bar{b})$. For $L = 50 \text{ fb}^{-1}$ and $R = 0.01\%, 0.06\%$, $G(b\bar{b})$ can be measured with an accuracy of $\pm 0.4\%, \pm 2\%$ ($\pm 3\%, \pm 15\%$) at $m_h = 110 \text{ GeV}$ ($m_h = m_Z$). By combining this measurement with the $\pm \sim 7\%$ determination of $BF(h \rightarrow b\bar{b})$ that could be made in the Zh production mode, a roughly $\pm 8 - 10\%$ determination of $\Gamma(h \rightarrow \mu^+\mu^-)$ becomes possible. ($R = 0.01\%$ is required if $m_h \sim m_Z$.)

Suppose we find a light Higgs h and measure its mass, total width and partial widths. The critical questions that then arise are:

- Can we determine if the particle is a SM Higgs or a supersymmetric Higgs?
- If the particle is a supersymmetric Higgs boson, say in the MSSM, can we then predict masses of the heavier Higgs bosons H^0, A^0 , and H^\pm in order to discover them in subsequent measurements?

In the context of the MSSM, the answers to these questions can be delineated.

Enhancements of Γ_h^{tot} of order 30% relative to the prediction for the SM h_{SM} are the norm (even neglecting possible SUSY decays) for $m_{A^0} \lesssim 400 \text{ GeV}$. A 10% measurement of Γ_h^{tot} would thus be relatively likely to reveal a 3σ statistical enhancement. However, using the deviation to determine the value of m_{A^0} is model-dependent. For example, if $m_h = 110 \text{ GeV}$ and there is no stop mixing, then the percentage deviation would fairly uniquely fix m_{A^0} , whereas if $m_h = 110 \text{ GeV}$ and there is maximal stop mixing, as defined in Ref. [14], then the measured deviation would only imply a relation between $\tan \beta$ and m_{A^0} .

Γ_h^{tot} could be combined with branching ratios to yield a more definitive determination of m_{A^0} . For instance, we can compute $\Gamma(h \rightarrow b\bar{b}) = \Gamma_h^{\text{tot}} BF(h \rightarrow b\bar{b})$ using $BF(h \rightarrow b\bar{b})$ as measured in Zh production. It turns out that the percentage deviation of this partial width for the h^0 from the h_{SM} prediction is rather independent of $\tan \beta$ and gives a mixing-independent determination of m_{A^0} , which, after including systematic uncertainties in our knowledge of m_b , would discriminate

between a value of $m_{A^0} \leq 300$ GeV vs. $m_{A^0} = \infty$ at the $\geq 3\sigma$ statistical level.

Returning to $\Gamma(h \rightarrow \mu^+\mu^-)$, deviations at the $\gtrsim 3\sigma$ statistical level in the prediction for this partial width for the h^0 as compared to the h_{SM} are predicted out to $m_{A^0} \gtrsim 400$ GeV. Further, the percentage of deviation from the SM prediction would provide a relatively accurate determination of m_{A^0} for $m_{A^0} \lesssim 400$ GeV. For example, if $m_h = 110$ GeV, $\Gamma(h^0 \rightarrow \mu^+\mu^-)$ changes by 20% (a $\gtrsim 2\sigma$ effect) as m_{A^0} is changed from 300 GeV to 365 GeV.

Deviations for other quantities, e.g. $BF(h \rightarrow b\bar{b})$, depend upon the details of the stop squark masses and mixings, the presence of SUSY decay modes, and so forth, much as described in the case of Γ_h^{tot} . Only partial widths provide a mixing-independent determination of m_{A^0} . The $\mu^+\mu^-$ collider provides, as described, at least two particularly unique opportunities for determining two very important partial widths, $\Gamma(h \rightarrow b\bar{b})$ and $\Gamma(h \rightarrow \mu^+\mu^-)$, thereby allowing a test of the predicted proportionality of these partial widths to fermion mass independent of the lepton/quark nature of the fermion.

Thus, if $m_{A^0} \lesssim 400$ GeV, we may gain some knowledge of m_{A^0} through precision measurements of the h^0 's partial widths. This would greatly facilitate direct observation of the A^0 and H^0 via s -channel production at a $\mu^+\mu^-$ collider with $\sqrt{s} \lesssim 500$ GeV. As discussed in more detail shortly, even without such pre-knowledge of m_{A^0} , discovery of the A^0, H^0 Higgs bosons would be possible in the s -channel at a $\mu^+\mu^-$ collider provided that $\tan\beta \gtrsim 3 - 4$. With pre-knowledge of m_{A^0} , detection becomes possible for $\tan\beta$ values not far above 1, provided $R \sim 0.01\%$ (crucial since the A^0 and H^0 become relatively narrow for low $\tan\beta$ values).

Other colliders offer various mechanisms to directly search for the A^0, H^0 , but also have limitations:

- The LHC has a discovery hole and “ h^0 -only” regions at moderate $\tan\beta$, $m_{A^0} \gtrsim 200$ GeV.
- At the NLC one can use the mode $e^+e^- \rightarrow Z^* \rightarrow H^0A^0$ (the mode h^0A^0 is suppressed for large m_{A^0}), but it is limited to $m_{H^0} \sim m_{A^0} \lesssim \sqrt{s}/2$.

- A $\gamma\gamma$ collider could probe heavy Higgs up to masses of $m_{H^0} \sim m_{A^0} \sim 0.8\sqrt{s}$, but this would quite likely require $L \sim 100 \text{ fb}^{-1}$, especially if the Higgs bosons are at the upper end of the $\gamma\gamma$ collider energy spectrum[20].

Most GUT models predict $m_{A^0} \gtrsim 200$ GeV, and perhaps as large as a TeV[21]. For large $m_{A^0} \sim m_{H^0}$, s -channel searches can be made at a $\mu^+\mu^-$ collider up to $\sim \sqrt{s}$, whereas the $Z^* \rightarrow H^0A^0$ mode at an e^+e^- collider fails for $m_{A^0} \sim m_{H^0} \gtrsim \sqrt{s}/2$. In particular, at a muon collider with $\sqrt{s} \sim 500$ GeV, scan detection of the A^0, H^0 is possible in the mass range from 200 to 500 GeV in s -channel production, provided $\tan\beta \gtrsim 3 - 4$, whereas an e^+e^- collider of the same energy can only probe $m_{H^0} \sim m_{A^0} \lesssim 220$ GeV. That the signals become viable when $\tan\beta > 1$ (as favored by GUT models) is due to the fact that the couplings of A^0 and (once $m_{A^0} \gtrsim 150$ GeV) H^0 to $b\bar{b}$ and, especially to $\mu^+\mu^-$, are proportional to $\tan\beta$, and thus increasingly enhanced as $\tan\beta$ rises.

Although the $\mu^+\mu^-$ collider cannot discover the H^0, A^0 in the $\tan\beta \lesssim 3$ region, this is a range in which the LHC *could* find the heavy Higgs bosons in a number of modes. That the LHC and the NMC are complementary in this respect is a very crucial point. Together, discovery of the A^0, H^0 is essentially guaranteed.

If the H^0, A^0 are observed at the $\mu^+\mu^-$ collider, measurement of their widths will typically be straightforward. For moderate $\tan\beta$ the A^0 and H^0 resonance peaks do not overlap and $R \lesssim 0.06\%$ will be adequate, since for such R values $\Gamma_{H^0, A^0} \gtrsim \sigma_{\sqrt{s}}$. However, if $\tan\beta$ is large, then for most of the $m_{A^0} \gtrsim 200$ GeV parameter range the A^0 and H^0 are sufficiently degenerate that there is significant overlap of the A^0 and H^0 resonance peaks. In this case, $R \sim 0.01\%$ resolution would be necessary for observing the double-peaked structure and separating the A^0 and H^0 resonances.

A $\sqrt{s} \sim 500$ GeV muon collider still might not have sufficient energy to discover heavy supersymmetric Higgs bosons. Further, distinguishing the MSSM from the SM by detecting small deviations of the h^0 properties from those predicted for the h_{SM} becomes quite difficult for $m_{A^0} \gtrsim 400$ GeV. However, construction of a

higher energy machine, say $\sqrt{s} = 4$ TeV, would allow discovery of A^0, H^0 in the $b\bar{b}$ or $t\bar{t}$ channels (see the discussion in Section 5).

We close this section with brief comments on the effects of bremsstrahlung and beam polarization. Soft photon radiation must be included when determining the resolution in energy and the peak luminosity achievable at an e^+e^- or $\mu^+\mu^-$ collider. This radiation is substantially reduced at a $\mu^+\mu^-$ collider due to the increased mass of the muon compared to the electron. In Fig. 6 we show the luminosity distribution before and after including the soft photon radiation. These bremsstrahlung effects are calculated in Ref. [16]. A long tail extends down to low values of the energy.

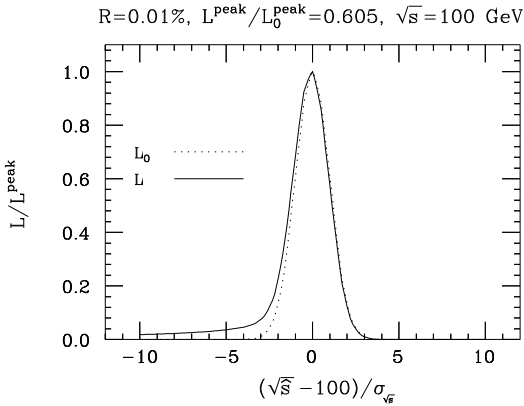


Figure 6: $d\mathcal{L}/d\sqrt{\hat{s}}$ relative to its peak value at $\sqrt{\hat{s}} = \sqrt{s}$ is plotted before and after soft-photon radiation. We have taken $\sqrt{s} = 100$ GeV and $R = 0.01\%$. The ratio of peak height after including soft-photon radiation to that before is 0.605.

For a SM-like Higgs boson with width smaller than $\sigma_{\sqrt{s}}$, the primary effect of bremsstrahlung is a reduction in the peak luminosity. The ratio of the luminosity peak height after and before including the bremsstrahlung is shown in Fig. 7. The conclusions above regarding s -channel Higgs detection are those obtained with inclusion of bremsstrahlung effects.

The low-energy bremsstrahlung tail provides a self-scan over the range of energies below the design energy, and thus can be used to detect s -channel resonances. The full luminosity distri-

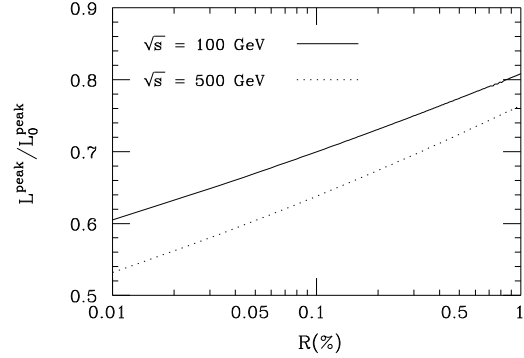


Figure 7: $\left. \frac{d\mathcal{L}}{d\sqrt{\hat{s}}} / \frac{d\mathcal{L}_0}{d\sqrt{\hat{s}}} \right|_{\sqrt{\hat{s}}=\sqrt{s}}$ as a function of R for $\sqrt{s} = 100$ and 500 GeV.

bution for the tail is shown in Fig. 8. Observation of A^0, H^0 peaks in the $b\bar{b}$ mass distribution $m_{b\bar{b}}$ created by this bremsstrahlung tail may be possible. The region of the $(m_{A^0}, \tan\beta)$ parameter space plane for which a peak is observable depends strongly on the $b\bar{b}$ invariant mass resolution. For an excellent $m_{b\bar{b}}$ mass resolution of order ± 5 GeV and integrated luminosity of $L = 50 \text{ fb}^{-1}$ at $\sqrt{s} = 500$ GeV, the A^0, H^0 peak(s) are observable for $\tan\beta \gtrsim 5$ at $m_{A^0} \gtrsim 400$ GeV (but only for very large $\tan\beta$ values in the $m_{A^0} \sim m_Z$ region due to the large s -channel Z contribution to the $b\bar{b}$ background).

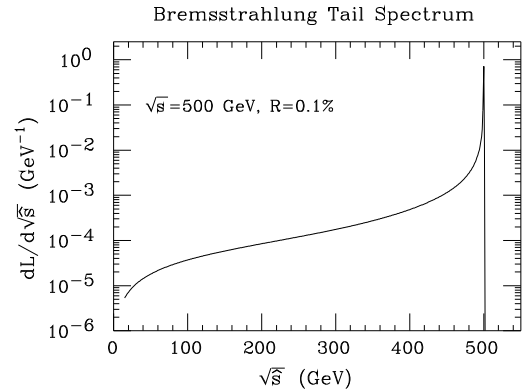


Figure 8: $\frac{d\mathcal{L}}{d\sqrt{\hat{s}}}$ as a function of $\sqrt{\hat{s}}$ for $R = 0.1\%$ and $\sqrt{s} = 500$ GeV. The integral under the curve is normalized to 1.

In the s -channel Higgs studies, polarization of the muon beams could present a significant advantage over the unpolarized case, since signal and background come predominantly from different polarization states. Polarization P of both beams would enhance the significance of a Higgs signal provided the factor by which the luminosity is reduced is not larger than $(1 + P^2)^2/(1 - P^2)$. For example, a reduction in luminosity by a factor of 10 could be compensated by a polarization $P = 0.84$, leaving the significance of the signal unchanged[22]. Furthermore, *transverse* polarization of the muon beams could prove useful for studying CP-violation in the Higgs sector. Muons are produced naturally polarized from π and K decays. An important consideration for the future design of muon colliders is the extent to which polarization can be maintained through the cooling and acceleration processes.

3. PRECISION THRESHOLD STUDIES

Good beam energy resolution is crucial for the determination of the Higgs width. Another area of physics where the naturally good resolution of a $\mu^+\mu^-$ collider would prove valuable is studies of the $t\bar{t}$ and W^+W^- thresholds, similar to those proposed for the NLC and LEP II. The $t\bar{t}$ threshold shape determines m_t , Γ_t and the strong coupling α_s , while the W^+W^- threshold shape determines m_W and possibly also Γ_W . At a $\mu^+\mu^-$ collider, even a conservative natural beam resolution $R \sim 0.1\%$ would allow substantially increased precision in the measurement of most of these quantities as compared to other machines. Not only is such monochromaticity already greatly superior to e^+e^- collider designs, where typically $R \sim 1\%$, but also at a $\mu^+\mu^-$ collider there is no significant beamstrahlung and the amount of initial state radiation (ISR) is greatly reduced. ISR and, especially, beam smearing cause significant loss of precision in the measurement of the top quark and W masses at e^+e^- colliders.

To illustrate, consider threshold production of the top quark, which has been extensively studied for e^+e^- colliders[24]. Figure 9 shows the effects of including beam smearing and ISR for the threshold production of top quarks using a Gaussian beam spread of 1% for the e^+e^- collider[25].

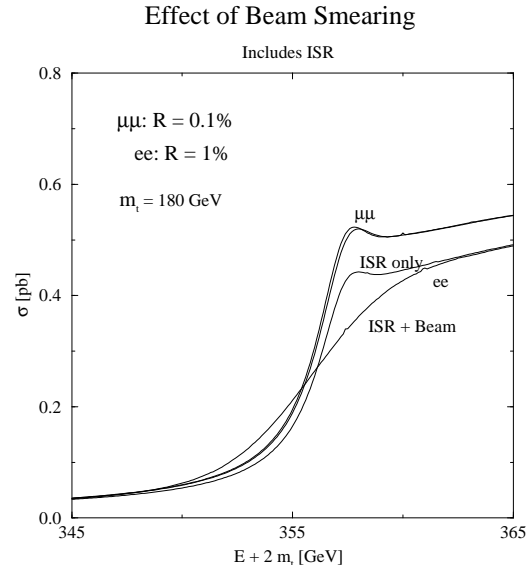


Figure 9: The threshold curves are shown for $\mu^+\mu^-$ and e^+e^- machines including ISR and with and without beam smearing. Beam smearing has only a small effect at a muon collider, whereas at an electron collider the threshold region is significantly smeared. The strong coupling is taken to be $\alpha_s(m_Z) = 0.12$.

Also shown are our corresponding results for the $\mu^+\mu^-$ collider with $R = 0.1\%$, see [25]. The threshold peak is no longer washed out in the $\mu^+\mu^-$ case. The precision with which one could measure m_t , α_s and Γ_t at various facilities is shown in Table 1. Improvements in the determination of m_W should also be possible[23].

The value of such improvements in precision can be substantial. Consider precision electroweak corrections, for example. The prediction for the SM or SM-like Higgs mass m_h depends on m_W and m_t through the one-loop equation

$$m_W^2 = m_Z^2 \left[1 - \frac{\pi\alpha}{\sqrt{2}G_\mu m_W^2 (1 - \delta r)} \right]^{1/2}, \quad (25)$$

where δr depends quadratically on m_t and logarithmically on m_h . Current expectations for LEP II and the Tevatron imply precisions of order

$$\Delta m_W = 40 \text{ MeV}, \quad (26)$$

$$\Delta m_t = 4 \text{ GeV}. \quad (27)$$

Table 1: Measurements of the standard model parameters: top mass m_t , strong coupling α_s , and top quark width Γ_t .

	Tevatron (1000 pb^{-1}) (10 fb^{-1})	LHC (20 pb^{-1})	NLC (10 fb^{-1})	FMC (10 fb^{-1})
Δm_t (GeV)	4 1	2	0.52[26]	0.3
$\Delta\alpha_s$			0.009	0.008
$\Delta\Gamma_t/\Gamma_t$	0.3[27]		0.2	better

For the uncertainties of Eq. (27) and the current central values of $m_W = 80.4$ GeV and $m_t = 180$ GeV, the Higgs mass would be constrained to the 1σ range

$$50 < m_h < 200 \text{ GeV} . \quad (28)$$

In electroweak precision analyses, an error of $\Delta m_W = 40$ MeV is equivalent to an error of $\Delta m_t = 6$ GeV, so increased precision for m_W would be of greatest immediate interest given the $\Delta m_t = 4$ GeV error quoted above. In order to make full use of the $\Delta m_t \lesssim 0.5$ GeV precision possible at a $\mu^+\mu^-$ collider would require $\Delta m_W \lesssim 4$ MeV. We are currently studying the possibility that the latter can be achieved at a $\mu^+\mu^-$ collider.

Such precisions, combined with the essentially exact determination of m_h possible at a $\mu^+\mu^-$ collider, would allow a consistency test for precision electroweak measurements at a hitherto unimaginable level of accuracy. If significant inconsistency is found, new physics could be revealed. For example, inconsistency could arise if the light h is not that of the SM but rather the h^0 of the MSSM and there is a contribution to precision electroweak quantities arising from the H^0 of the MSSM having a non-negligible WW, ZZ coupling. The contributions of stop and chargino states to loops would be another example.

A precise determination of the top quark mass m_t could well be important in its own right. One scenario is that the low-energy spectrum of particles (SUSY or not) has been measured and there is a desert up to the GUT scale. We would then want to extrapolate the low-energy parameters up to the grand unified scale to test in a detailed way the physics at that scale. Then the top quark mass (and the Yukawa coupling) would

be crucially important since this parameter determines to a large extent the evolution of all the other Yukawas, including flavor mixings. These considerations become especially important if the top quark Yukawa coupling is determined by an infrared quasi-fixed point for which very small changes in the top quark mass translate into very large changes in the renormalized values of many other parameters in the theory.

4. CP VIOLATION AND FCNC IN THE HIGGS SECTOR

A nonstandard Higgs sector could have sizable CP-violating effects as well as new flavor changing neutral current (FCNC) effects that could be probed with a $\mu^+\mu^-$ collider. A general two Higgs doublet model has been studied in Refs. [29,30,31]. There one would either (i) measure correlations in the final state, or (ii) transversely polarize the muon beams to observe an asymmetry in the production rate as a function of spin orientation. For the second option, the ability to achieve transverse polarization with the necessary luminosity is a crucial consideration.

New FCNC effects could be studied as well[32]. For example a Higgs in the s -channel could exhibit the decay $\mu^+\mu^- \rightarrow H^0 \rightarrow t\bar{c}$. This decay would have to compete against the WW^* decays.

5. EXOTIC HIGGS BOSONS/SCALARS

In general, a muon collider can probe any type of scalar that has significant fermionic couplings. Interesting new physics could be revealed. To give one example, consider the possibility that a doubly-charged Higgs boson with lepton-number-

violating coupling $\Delta^{--} \rightarrow \ell^- \ell^-$ exists, as required in left-right symmetric models where the neutrino mass is generated by the see-saw mechanism through a vacuum expectation value of a neutral Higgs triplet field. Such a Δ^{--} could be produced in $\ell^- \ell^-$ collisions. This scenario was studied in Ref. [33] for an $e^- e^-$ collider, but a $\mu^- \mu^-$ collider would be even better due to the much finer energy resolution (which enhances cross sections) and the fact that the $\Delta^{--} \rightarrow \mu^- \mu^-$ coupling should be larger than the $\Delta^{--} \rightarrow e^- e^-$ coupling.

Most likely, a Δ^{--} in the $\lesssim 500$ GeV region would already be observed at the LHC by the time the muon collider begins operation. In some scenarios, it would even be observed to decay to $\mu^- \mu^-$ so that the required s -channel coupling would be known to be non-zero. However, the magnitude of the coupling would not be determined; for this we would need the $\mu^- \mu^-$ collider. In the likely limit where $\Gamma_{\Delta^{--}} \ll \sigma_{\sqrt{s}}$, the number of Δ^{--} events for $L = 50 \text{ fb}^{-1}$ is given by

$$N(\Delta^{--}) = 6 \times 10^{11} \left(\frac{c_{\mu\mu}}{10^{-5}} \right) \left(\frac{0.01\%}{R(\%)} \right), \quad (29)$$

where the standard Majorana-like coupling-squared is parameterized as

$$|h_{\mu\mu}|^2 = c_{\mu\mu} m_{\Delta^{--}}^2 (\text{GeV}). \quad (30)$$

Current limits on the coupling correspond to $c_{\mu\mu} \lesssim 5 \times 10^{-5}$. Assuming that 30 to 300 events would provide a distinct signal (the larger number probably required if the dominant Δ^{--} decay channel is into $\mu^- \mu^-$, for which there is a significant $\mu^- \mu^- \rightarrow \mu^- \mu^-$ background), the muon collider would probe some 11 to 10 orders of magnitude more deeply in the coupling-squared than presently possible. This is a level of sensitivity that would almost certainly be adequate for observing a Δ^{--} that is associated with the triplet Higgs boson fields that give rise to see-saw neutrino mass generation in the left-right symmetric models.

6. PHYSICS AT A $2 \otimes 2$ TEV $\mu^+ \mu^-$ COLLIDER

Bremsstrahlung radiation scales like m^{-4} , so a circular storage ring can be used for muons at

high energies. A high energy lepton collider with center-of-mass energy of 4 TeV would provide new physics reach beyond that contemplated at the LHC or NLC (with $\sqrt{s} \lesssim 1.5$ TeV). We concentrate primarily on the following scenarios for physics at these energies: (1) heavy supersymmetric (SUSY) particles, (2) strong scattering of longitudinal gauge bosons (generically denoted W_L) in the electroweak symmetry breaking (EWSB) sector, and (3) heavy vector resonance production, like a Z' .

6.1. SUSY Factory

Low-energy supersymmetry is a theoretically attractive extension of the Standard Model. Not only does it solve the naturalness problem, but also the physics remains essentially perturbative up to the grand unification scale, and gravity can be included by making the supersymmetry local. Since the SUSY-breaking scale and, hence, sparticle masses are required by naturalness to be no larger than 1 – 2 TeV, a high energy $\mu^+ \mu^-$ collider with $\sqrt{s} = 4$ TeV is guaranteed to be a SUSY factory if SUSY is nature's choice. Indeed, it may be the only machine that would guarantee our ability to study the full spectrum of SUSY particles. The LHC has sufficient energy to produce supersymmetric particles but disentangling the spectrum and measuring the masses will be a challenge due to the complex cascade decays and QCD backgrounds. The NLC would be a cleaner environment than the LHC to study the supersymmetric particle decays, but the problem here may be insufficient energy to completely explore the full particle spectrum.

Most supersymmetric models have a symmetry known as an R -parity that requires that supersymmetric particles be created or destroyed in pairs. This means that the energy required to find and study heavy scalars is more than twice their mass. (If R -parity is violated, then sparticles can also be produced singly; the single sparticle production rate would depend on the magnitude of the violation, which is model- and generation-dependent.) Further, a p -wave suppression is operative for the production of scalars (in this case the superpartners to the ordinary quarks and leptons), and energies well above the kinematic threshold might be required to produce the scalar pairs

at an observable rate, as illustrated in Fig. 10. In addition, a large lever arm for exploring the different threshold behaviour of spin-0 and spin-1/2 SUSY sparticles could prove useful in mass determinations.

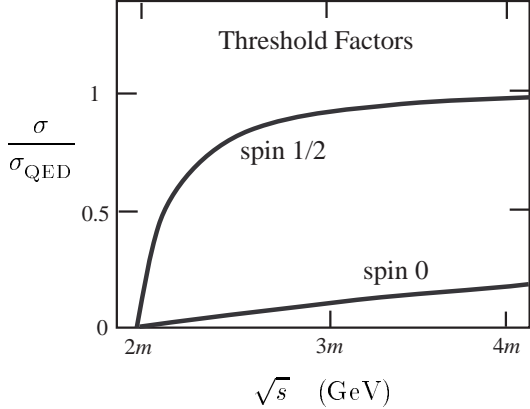


Figure 10: Comparison of kinematic suppression for fermion pairs and squark pair production at e^+e^- or $\mu^+\mu^-$ colliders.

To be more specific, it is useful to constrain the parameter space by employing a supergravity (SUGRA) model. Such models are particularly attractive in that the breaking of the electroweak symmetry is accomplished radiatively by the large top quark Yukawa coupling driving one of the Higgs doublet masses negative through renormalization group evolution. The simplest SUGRA models contain the following parameters:

- a universal scalar mass m_0 ;
- a universal gaugino mass $m_{1/2}$;
- the ratio of the electroweak scale Higgs vev's, $\tan\beta = v_2/v_1$;
- a universal trilinear term A_0 ;
- the sign of the Higgs mixing: $\text{sign}(\mu)$.

The parameters above are constrained by various means. Experimental bounds on the superpartner masses put a lower bound on $m_{1/2}$. Naturalness considerations yield upper bounds on both $m_{1/2}$ and m_0 , which, in turn, imply upper limits on the superparticle masses. If one supposes that the LSP is the cold dark matter of the universe,

then there is an upper limit on m_0 so that the annihilation channels for the LSP are not suppressed by the heavy scalar masses. The A_0 parameter is limited by the requirement of an acceptable vacuum state; $1 \lesssim \tan\beta \lesssim 50 - 60$ is required for perturbativity of the Yukawa couplings. A representative choice of parameters that is consistent with all these constraints, but at the same time illustrates the power of a $\mu^+\mu^-$ collider is:

$$\begin{aligned} m_0 &= 2m_{1/2} = 500 \text{ GeV} , \\ \tan\beta &= 2, \quad A_0 = 0, \quad \mu < 0 . \end{aligned} \quad (31)$$

By adopting a large ratio of $m_0/m_{1/2} = 2$ the scalars become heavy (with the exception of the lightest Higgs boson) compared to the gauginos. The particle and sparticle masses obtained from renormalization group evolution are:

$$m_{h^0} = 88 \text{ GeV}, \quad m_{A^0} = 921 \text{ GeV} , \quad (32)$$

$$m_{H^\pm} = m_{H^0} = 924 \text{ GeV} , \quad (33)$$

$$m_{\tilde{q}_L} \simeq 752 \text{ GeV}, \quad m_{\tilde{q}_R} \simeq 735 \text{ GeV} , \quad (34)$$

$$m_{\tilde{b}_1} = 643 \text{ GeV}, \quad m_{\tilde{b}_2} = 735 \text{ GeV} , \quad (35)$$

$$m_{\tilde{t}_1} = 510 \text{ GeV}, \quad m_{\tilde{t}_2} = 666 \text{ GeV} , \quad (36)$$

$$m_{\tilde{\nu}} \sim m_{\tilde{\ell}} \sim 510 - 530 \text{ GeV} , \quad (37)$$

$$m_{\tilde{\chi}_{1,2,3,4}^0} = 107, 217, 605, 613 \text{ GeV} , \quad (38)$$

$$m_{\tilde{\chi}_{1,2}^\pm} = 217, 612 \text{ GeV} . \quad (39)$$

Thus, the choice of GUT parameters, Eq. (31), leads, as desired, to a scenario such that pair production of heavy scalars is only accessible at a high energy machine like the NMC.

First, we consider the pair production of the heavy Higgs bosons

$$\mu^+\mu^- \rightarrow Z \rightarrow H^0 A^0 , \quad (40)$$

$$\mu^+\mu^- \rightarrow \gamma, Z \rightarrow H^+ H^- . \quad (41)$$

The cross sections are shown in Fig. 11 versus \sqrt{s} . A $\mu^+\mu^-$ collider with $\sqrt{s} \gtrsim 2 \text{ TeV}$ is needed and well above the threshold the cross section is $\mathcal{O}(1 \text{ fb})$. In the scenario of Eq. (31), the decays of these heavy Higgs bosons are predominantly into top quark modes ($t\bar{t}$ for the neutral Higgs and $t\bar{b}$ for the charged Higgs), with branching fractions near 90%. Observation of the H^0 , A^0 , and H^\pm would be straightforward even for a pessimistic luminosity of $L = 100 \text{ fb}^{-1}$. Backgrounds would be negligible once the requirement

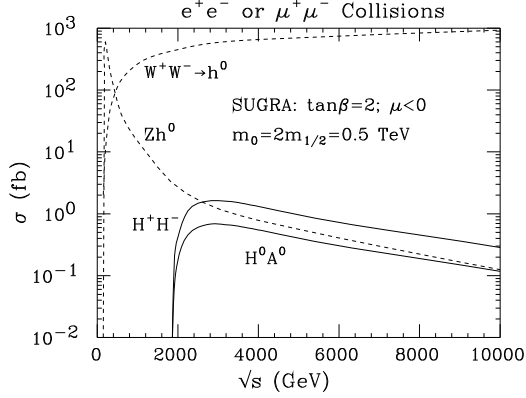


Figure 11: Pair production of heavy Higgs bosons at a high energy lepton collider. For comparison, cross sections for the lightest Higgs boson production via the Bjorken process $\mu^+\mu^- \rightarrow Z^* \rightarrow Zh^0$ and via the WW fusion are also presented.

of roughly equal masses for two back-to-back particles is imposed.

In other scenarios the decays may be more complex and include multiple decay modes into supersymmetric particles, in which case the overall event rate might prove crucial to establishing a signal. In some scenarios investigated in Ref. [34] complex decays are important, but the $\mu^+\mu^-$ collider has sufficient production rate that one or more of the modes

$$(H^0 \rightarrow b\bar{b}) + (A^0 \rightarrow b\bar{b}), \quad (42)$$

$$(H^0 \rightarrow h^0 h^0 \rightarrow b\bar{b}b\bar{b}) + (A^0 \rightarrow X), \quad (43)$$

$$(H^0 \rightarrow t\bar{t}) + (A^0 \rightarrow t\bar{t}), \quad (44)$$

are still visible above the backgrounds for $L \gtrsim 500 \text{ fb}^{-1}$. Despite the significant dilution of the signal by the additional SUSY decay modes (which is most important at low $\tan\beta$), one can observe a signal of $\gtrsim 50$ events in one channel or another.

The high energy $\mu^+\mu^-$ collider will yield a large number of the light SM-like h^0 via $\mu^+\mu^- \rightarrow Z^* \rightarrow Zh^0$ and WW fusion, $\mu^+\mu^- \rightarrow \nu\bar{\nu}h^0$. In contrast to a machine running at FMC energies ($\sqrt{s} \sim 500 \text{ GeV}$), where the cross sections for these two processes are comparable, at higher energies, $\sqrt{s} \gtrsim 1 \text{ TeV}$, the WW fusion process dominates as shown in Fig. 11.

Any assessment of the physics signals in the pair production of the supersymmetric partners of the quarks and leptons is model-dependent. However, as illustrated by the specific SUGRA scenario masses of Eq. (39), squarks are expected to be somewhat heavier than the sleptons due to their QCD interactions which affect the running of their associated ‘soft’ masses away from the universal mass m_0 in the evolution from the GUT scale to low energies. Except for the LSP, the lightest superpartner of each type decays to a gaugino (or gluino) and an ordinary fermion, and the gaugino will decay if it is not the LSP. Since the particles are generally too short-lived to be observed, we must infer everything about their production from their decay products.

We illustrate the production cross sections for several important sparticle pairs in Fig. 12 for the SUGRA model of Eq. (31). For a collider with $\sqrt{s} \sim 4 \text{ TeV}$, cross sections of $\sim 2\text{--}30 \text{ fb}$ are expected.

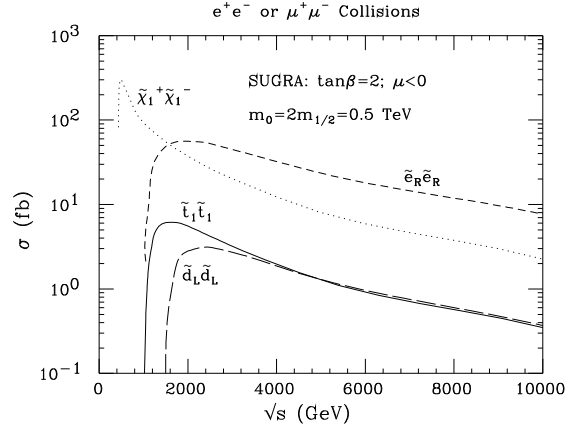


Figure 12: The production cross sections for SUSY particles in a supergravity model with heavy scalars.

The final states of interest are determined by the dominant decay modes, which in this model are $\tilde{e}_R \rightarrow e\tilde{\chi}_1^0$ ($BF = 0.999$), $\tilde{\chi}_1^+ \rightarrow W^+\tilde{\chi}_1^0$ ($BF = 0.999$), $\tilde{d}_L \rightarrow \tilde{\chi}_1^- u$, $\tilde{\chi}_2^0 d$, $\tilde{g}d$ ($BF = 0.52, 0.27, 0.20$), and $\tilde{t}_1 \rightarrow \tilde{\chi}_1^+ t$. Thus, for example, with a luminosity of $L = 200 \text{ fb}^{-1}$ at $\sqrt{s} = 4 \text{ TeV}$, \tilde{d}_L pair production would result in $200 \times 2 \times (0.52)^2 = 100$ events containing two u -quark jets, two ener-

getic leptons (not necessarily of the same type), and substantial missing energy. The SM background should be small, and the signal would be clearly visible. The energy spectra of the quark jets would allow a determination of $m_{\tilde{d}_L} - m_{\tilde{\chi}_1^+}$ while the lepton energy spectra would fix $m_{\tilde{\chi}_1^+} - m_{\tilde{\chi}_1^0}$. If the machine energy can be varied, then the turn-on of such events would fix the \tilde{d}_L mass. The $\tilde{\chi}_1^+$ and $\tilde{\chi}_1^0$ masses would presumably already be known from studying the $\ell^+\ell^-$ +missing-energy signal from $\tilde{\chi}_1^+\tilde{\chi}_1^-$ pair production, best performed at much lower energies. Thus, cross checks on the gaugino masses are possible, while at the same time two determinations of the \tilde{d}_L mass become available (one from threshold location and the other via the quark jet spectra combined with a known mass for the $\tilde{\chi}_1^+$).

This example illustrates the power of a $\mu^+\mu^-$ collider, especially one whose energy can be varied over a broad range. Maintaining high luminosity over a broad energy range may require the construction of several (relatively inexpensive) final storage rings.

6.2. The $W_L W_L \rightarrow W_L W_L$ probe of EWSB

A compelling motivation for building any new machine is to discover the mechanism behind EWSB. This may involve directly producing the Higgs particle of the Standard Model or supersymmetric particles. Alternatively it could be that no light Higgs bosons exist; then general arguments based on partial wave unitarity require that the interactions of the longitudinal gauge bosons (W and Z) become strong and nonperturbative. The energy scale where this happens is about 1–2 TeV, implying that a collider needs to probe vector boson scattering at energies at least this high. The LHC energy and the currently envisioned NLC energies (up to ~ 1.5 TeV) are marginally able to do this. In contrast, a 4 TeV muon collider is in the optimal energy range for a study of strong vector boson scattering. The construction of a multi-TeV e^+e^- collider is also a possibility[36].)

Strong electroweak scattering (SEWS) effects can be estimated by using the Standard Model with a heavy Higgs as a prototype of the strong scattering sector. The SM with a light Higgs is

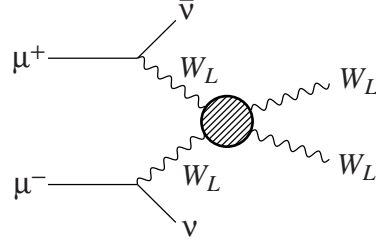


Figure 13: Symbolic diagram for strong WW scattering.

an appropriate definition of the electroweak background since only transversely polarized W 's contribute to vector boson scattering when the Higgs has a small mass. For a 1 TeV SM Higgs boson, the signal is thus defined as

$$\Delta\sigma = \sigma(m_{h_{SM}} = 1 \text{ TeV}) - \sigma(m_{h_{SM}} = 10 \text{ GeV}) . \quad (45)$$

Results for $\Delta\sigma$ are shown in Table 2 for $\sqrt{s} = 1.5$ TeV (possibly the upper limit for a first e^+e^- collider) and 4 TeV. The strong scattering signal is relatively small at energies of order 1 TeV, but grows substantially as multi-TeV energies are reached. Thus, the highest energies in \sqrt{s} that can be reached at a muon collider could be critically important.

Table 2: Strong electroweak scattering signals in $W^+W^- \rightarrow W^+W^-$ and $W^+W^- \rightarrow ZZ$ at future lepton colliders.

\sqrt{s}	$\Delta\sigma(W^+W^-)$	$\Delta\sigma(ZZ)$
1.5 TeV	8 fb	6 fb
4 TeV	80 fb	50 fb

Many other models for the strongly interacting gauge sector have been constructed in addition to the SM, including[37]:

- a (“Scalar”) model in which there is a scalar Higgs resonance with $M_S = 1$ TeV but non-SM width of $\Gamma_S = 350$ GeV;
- a (“Vector”) model in which there is no scalar resonance, but rather a vector resonance with $M_V = 1$ TeV and $\Gamma_V = 35$ GeV;

- a model, denoted by “LET” or “ $m_{h_{SM}} = \infty$ ”, in which the SM Higgs is taken to have infinite mass and the partial waves simply follow the behavior predicted by the low-energy theorems;
- a model (denoted by “LET-K”) in which the LET behavior is unitarized via K -matrix techniques.

To differentiate among models, a complete study of the physics of strongly interacting gauge bosons would be required. In particular, all the following vector-boson scattering channels must be studied:

$$W^+W^- \rightarrow W^+W^-, ZZ, \quad (46)$$

$$W^\pm Z \rightarrow W^\pm Z, \quad (47)$$

$$W^\pm W^\pm \rightarrow W^\pm W^\pm. \quad (48)$$

Partial exploration of the three isospin channels can be made at the LHC. The signal and background for gold-plated (purely leptonic) events is shown in Table 3 for the LHC operating at 14 TeV with $L = 100 \text{ fb}^{-1}$, for several of the above models. These channels have also been studied for a 1.5 TeV NLC[38], and, again, event rates are at a level that first signals of the strongly interacting vector boson sector would emerge, but the ability to discriminate between models and actually study these strong interactions would be limited.

Table 3: Total numbers of $W_L W_L \rightarrow 4\text{-lepton}$ signal S and background B events calculated for the LHC[37], assuming $L = 100 \text{ fb}^{-1}$.

	Bkgd	Scalar	Vector	LET-K
$ZZ(4\ell)$	1	5	1.5	1.5
$(2\ell 2\nu)$	2	17	5	4.5
W^+W^-	12	18	6	5
W^+Z	22	2	70	3
$W^\pm W^\pm$	4	7	12	13

For a $\mu^+\mu^-$ collider operating at 4 TeV the statistical significances markedly improve. Table 4 summarizes the total signal S and background B event numbers, summing over diboson invariant mass bins, together with the statistical significance S/\sqrt{B} for different models of the strongly-interacting physics. A broad Higgs-like scalar will enhance both W^+W^- and ZZ

channels with $\sigma(W^+W^-) > \sigma(ZZ)$; a ρ -like vector resonance will manifest itself through W^+W^- but not ZZ ; while the $m_{h_{SM}} = \infty$ (LET) amplitude will enhance ZZ more than W^+W^- . The $m_{h_{SM}} = \infty$ signal for W^+W^- is visible, although still far from robust; the ratio S/B can be enhanced by making a higher mass cut (*e.g.* $M_{WW} > 0.7 \text{ TeV}$), but the significance S/\sqrt{B} is not improved.

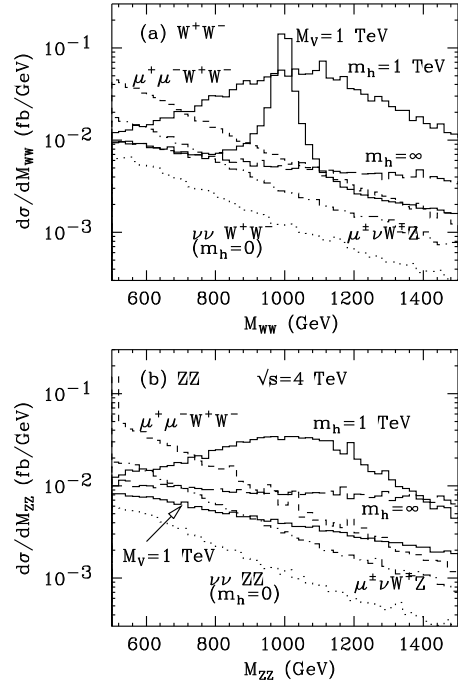


Figure 14: Histograms for the signals and backgrounds in strong vector boson scattering in the (a) W^+W^- and (b) ZZ final states. The background is given by the strictly electroweak $m_{h_{SM}} = 0$ limit of the Standard Model. The three signals shown are (I) a vector resonance with $M_V = 1 \text{ TeV}$, $\Gamma_V = 35 \text{ GeV}$, (II) the SM Higgs with $m_{h_{SM}} = 1 \text{ TeV}$, and (III) the SM with $m_{h_{SM}} = \infty$ (LET model). In the figure the shorthand notation h is used for h_{SM} .

Signals and the irreducible electroweak background for the W^+W^- and ZZ modes are shown in Fig. 14. The complementarity of these two modes is clear from the figure. However, to make use of this complementarity it is crucial to be able to distinguish final state W and Z bosons using the dijet invariant masses. This is possible pro-

Table 4: Total numbers of W^+W^- , $ZZ \rightarrow$ 4-jet signal S and background B events calculated for a 4 TeV $\mu^+\mu^-$ collider with integrated luminosity 200 fb^{-1} . Events are summed over the mass range $0.5 < M_{WW} < 1.5 \text{ TeV}$ except for the W^+W^- channel with a narrow vector resonance for which $0.9 < M_{WW} < 1.1 \text{ TeV}$. The statistical significance S/\sqrt{B} is also given. The hadronic branching fractions of WW decays and the W^\pm/Z identification/misidentification are included.

channels	SM $m_{h_{SM}} = 1 \text{ TeV}$	Scalar $M_S = 1 \text{ TeV}$	Vector $M_V = 1 \text{ TeV}$	SM $m_{h_{SM}} = \infty$
$S(\mu^+\mu^- \rightarrow \bar{\nu}\nu W^+W^-)$	1900	1400	370	230
$B(\text{backgrounds})$	1100	1100	110	1100
S/\sqrt{B}	57	42	35	6.9
$S(\mu^+\mu^- \rightarrow \bar{\nu}\nu ZZ)$	970	700	220	350
$B(\text{backgrounds})$	160	160	160	160
S/\sqrt{B}	77	55	17	28

vided there is sufficient jet energy resolution, as discussed in Ref. [38].

Finally, we note that event numbers in the 1 TeV SM Higgs and Vector resonance cases, and possibly even in the $m_{h_{SM}} = \infty$ (LET) case, are such that not only could a substantial overall signal be observed, but also at high L the shape of the excess, due to strong interactions, in the distribution in vector boson pair mass could be measured over a broad interval in the 1 TeV range. For instance, from Fig. 14a in the case of $m_{h_{SM}} = \infty$, a 100 GeV interval from 1.4 TeV to 1.5 TeV would contain $L \times 100 \text{ GeV} \times (4 \times 10^{-3} \text{ fb/GeV}) = 400$ signal events for $L = 1000 \text{ fb}^{-1}$, thereby allowing a 5% measurement of the $m_{W^+W^-}$ signal distribution in this bin. The level of accuracy in this one bin alone would distinguish this model from the Vector or $m_{h_{SM}} = 1 \text{ TeV}$ models. The difference between the three different distributions plotted in Fig. 14 could be tracked in both channels. The ability to measure the distributions with reasonable precision would allow detailed insight into the dynamics of the strongly interacting electroweak sector when the collider achieves energies substantially above 1 TeV. Thus, if some signals for a strongly interacting sector emerge at the LHC, a $\sqrt{s} = 3 - 4 \text{ TeV}$ $\mu^+\mu^-$ (or e^+e^- , if possible) collider will be essential.

6.3. Exotic Heavy States

The very high energy of a 4 TeV collider would open up the possibility of directly producing many new particles outside of the Standard Model. Some

exotic heavy particles that could be discovered and studied at a muon collider are (1) sequential fermions, $Q\bar{Q}$, $L\bar{L}$ [39], (2) lepto-quarks, (3) vector-like fermions[40], and (4) new gauge bosons like a Z' or W_R [41].

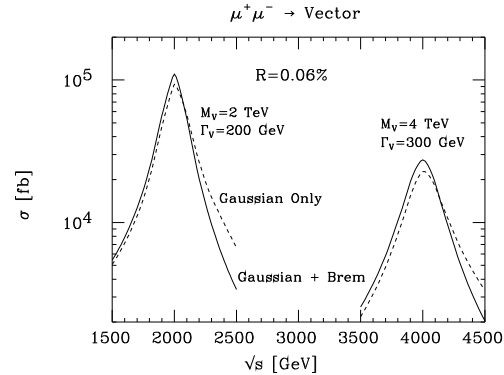


Figure 15: High event rates are possible if the muon collider energy is set equal to the vector resonance (Z' or ρ_{TC}) mass. Two examples are shown here with $R = 0.06\%$.

A new vector resonance such as a Z' or a technirho, ρ_{TC} , is a particularly interesting possibility. The collider could be designed to sit on the resonance $\sqrt{s} \sim M_V$ in which case it would function as a Z' or ρ_{TC} factory as illustrated in Fig. 15. Alternatively, if the mass of the resonance is not known a priori, then the collider operating at an energy above the resonance mass

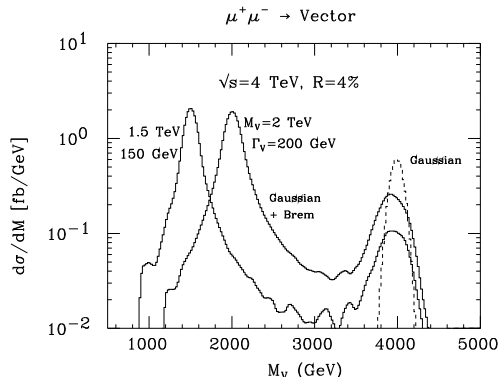


Figure 16: A heavy vector resonance can be visible in the bremsstrahlung tail of a high energy collider. Here a $\mu^+\mu^-$ collider operating at 4 TeV is shown for $M_V = 1.5$ TeV and 2 TeV.

could discover it via the bremsstrahlung tail shown in Fig. 8. Figure 16 shows the differential cross section in the reconstructed final state mass M_V for a muon collider operating at 4 TeV for two cases where the vector resonance has mass 1.5 TeV and 2 TeV. Dramatic and unmistakable signals would appear even for integrated luminosity as low as $L \gtrsim 50 - 100 \text{ fb}^{-1}$.

7. CONCLUSIONS

A muon collider is very likely to add substantially to our knowledge of physics in the coming decades. A machine with energy in the range $\sqrt{s} = 100\text{--}500$ GeV is comparable to the NLC and provides valuable additional features. The most notable of these is the possibility of creating a Higgs boson in the s -channel and measuring its mass and decay widths directly and precisely. Even if a light Higgs does not exist, studies of the $t\bar{t}$ and W^+W^- thresholds at such a low-energy machine would yield higher precision in determining m_t and m_W than possible at other colliders. A $\mu^+\mu^-$ collider with energy as high as $\sqrt{s} \sim 4$ TeV appears to be entirely feasible and is ideally suited for studying a strongly-interacting symmetry breaking sector, since the center-of-mass energy is well above the energy

range at which vector boson interactions must become strong. Many other types of exotic physics beyond the Standard Model could be probed at such a high machine energy. For example, if supersymmetry exists, a 4 TeV $\mu^+\mu^-$ collider would be a factory for sparticle pair production. Observation of a heavy Z' in the bremsstrahlung luminosity tail would be straightforward and the machine energy could later be reset to provide a Z' factory. All the issues presented in this paper will be discussed in greater detail in a forthcoming review article[9].

ACKNOWLEDGMENTS

This work was supported in part by the U.S. Department of Energy under Grants No. DE-FG02-95ER40896, No. DE-FG03-91ER40674 and No. DE-FG02-91ER40661. Further support was provided by the University of Wisconsin Research Committee, with funds granted by the Wisconsin Alumni Research Foundation, and by the Davis Institute for High Energy Physics.

REFERENCES

1. *Proceedings of the First Workshop on the Physics Potential and Development of $\mu^+\mu^-$ Colliders*, Napa, California (1992), Nucl. Instru. and Meth. **A350**, 24 (1994).
2. *Proceedings of the Second Workshop on the Physics Potential and Development of $\mu^+\mu^-$ Colliders*, Sausalito, California (1994), ed. by D. Cline, American Institute of Physics Conference Proceedings 352.
3. *Proceedings of the 9th Advanced ICFA Beam Dynamics Workshop: Beam Dynamics and Technology Issues for $\mu^+\mu^-$ Colliders*, Montauk, Long Island, (1995), to be published.
4. These proceedings.
5. R.B. Palmer and A. Tollestrup, unpublished report.
6. D.V. Neuffer, Ref. [2], p. 22.
7. D.V. Neuffer and R.B. Palmer, Ref. [2], p. 70.
8. V. Barger, M.S. Berger, K. Fujii, J.F. Gunion, T. Han, C. Heusch, W. Hong,

- S.K. Oh, Z. Parsa, S. Rajpoot, R. Thun and B. Willis, *Physics Goals of a $\mu^+\mu^-$ Collider*, appearing in Ref. [2], p. 55, hep-ph/9503258.
9. V. Barger, M. Berger, J.F. Gunion, T. Han, and R. Phillips, in preparation.
 10. G.P. Jackson and D. Neuffer, private communications.
 11. P. Janot, *Proceedings of the 2nd International Workshop on "Physics and Experiments with Linear e^+e^- Colliders"*, eds. F. Harris, S. Olsen, S. Pakvasa and X. Tata, Waikoloa, HI (1993), World Scientific Publishing, p. 192, and references therein; T. Barklow and D. Burke, private communication.
 12. See "JLC-I", KEK-92-16, December 1992.
 13. K. Kawagoe, *Proceedings of the 2nd International Workshop on "Physics and Experiments with Linear e^+e^- Colliders"*, eds. F. Harris, S. Olsen, S. Pakvasa and X. Tata, Waikoloa, HI (1993), World Scientific Publishing, p. 660.
 14. J.F. Gunion, A. Stange, and S. Willenbrock, preprint UCD-95-28 (1995), hep-ph/9602238, to be published in *Electroweak Physics and Beyond the Standard Model*, World Scientific Publishing Co., eds. T. Barklow, S. Dawson, H. Haber, and J. Siegrist.
 15. V. Barger, M. Berger, J.F. Gunion, and T. Han, Phys. Rev. Lett. **75**, 1462 (1995).
 16. V. Barger, M. Berger, J.F. Gunion, and T. Han, UCD-96-6, hep-ph/9602415.
 17. R.B. Palmer, private communication.
 18. H. Haber, R. Hempfling and A. Hoang, CERN-TH/95-216.
 19. M. Carena, J.R. Espinosa, M. Quiros and C.E.M. Wagner, Phys. Lett. **B355**, 209 (1995); J.A. Casas, J.R. Espinosa, M. Quiros and A. Riotto, Nucl. Phys. **B436**, 3 (1995).
 20. J.F. Gunion and H.E. Haber, Phys. Rev. **D48**, 5109 (1993).
 21. See, for example, R. Arnowitt and P. Nath, Phys. Rev. **69**, 725 (1992); Phys. Lett. **B289**, 368 (1992); G. G. Ross and R. G. Roberts, Nucl. Phys. **B377**, 571 (1992); S. Kelley, J. L. Lopez, D. V. Nanopoulos, H. Pois, and K. Yuan, Nucl. Phys. **B398**, 3 (1993); M. Drees and M. M. Nojiri, Phys. Rev. **D47**, 376 (1993); M. Olechowski and S. Pokorski, Nucl. Phys. **B404**, 590 (1993); D. J. Castaño, E. J. Piard, and P. Ramond, Phys. Rev. **D49**, 4882 (1994); V. Barger, M.S. Berger, and P. Ohmann, Phys. Rev. **D49**, 4908 (1994); M. Carena, M. Olechowski, S. Pokorski, and C.E.M. Wagner, Nucl. Phys. **B419**, 213 (1994); G. Kane, C. Kolda, and J. Wells, Phys. Rev. **D49**, 6173 (1994); W. de Boer, R. Ehret, and D.I. Kazakov, Z. Phys. **C67**, 647 (1995); M. Carena and C.E.M. Wagner, Nucl. Phys. **B452**, 45 (1995); S.F. King and P. White, Phys. Rev. **D52**, 4183 (1995).
 22. Z. Parsa (unpublished).
 23. S. Dawson, appearing in Ref. [3], hep-ph/9512260.
 24. For discussions of the $t\bar{t}$ threshold behavior at e^+e^- colliders, see V.S. Fadin and V.A. Khoze, JETP Lett. **46** 525 (1987); Sov. J. Nucl. Phys. **48** 309 (1988); M. Peshkin and M. Strassler, Phys. Rev. **D43**, 1500 (1991); G. Bagliesi, *et al.*, CERN Orange Book Report CERN-PPE/92-05; Y. Sumino, *et al.*, Phys. Rev. **D47**, 56 (1992); M. Jezabek, J.H. Kühn, T. Teubner, Z. Phys. **C56**, 653 (1992).
 25. M.S. Berger, talk presented at the *Workshop on Particle Theory and Phenomenology: Physics of the Top Quark*, Iowa State University, May 25–26, 1995, hep-ph/9508209.
 26. P. Igo-Kemenes, M. Martinez, R. Miquel and S. Orteu, CERN-PPE/93-200, Contribution to the *Workshop on Physics with Linear e^+e^- Colliders at 500 GeV*, K. Fujii, T. Matsui, and Y. Sumino, Phys. Rev. **D50**, 4341 (1994).
 27. C.P. Yuan, talk presented at *Int. Workshop on Elementary Particle Physics: Present and Future*, Valencia, Spain, June 5–9, 1995, hep-ph/9509209.
 28. F. Merritt, H. Montgomery, A. Sirlin and

- M. Swartz, *Precision Tests of Electroweak Physics*, report of the DPF Committee on Long Term Planning, 1994.
29. B. Grzadkowski and J.F. Gunion, Phys. Lett. **B350**, 218 (1995).
 30. D. Atwood and A. Soni, Phys. Rev. **D52**, 6271 (1995).
 31. A. Pilaftsis, Rutherford preprint RAL-TR/96-021.
 32. D. Atwood, L Reina and A. Soni, Phys. Rev. Lett. **75**, 3800 (1995).
 33. J.F. Gunion, preprint UCD-95-36, hep-ph/9510350, to be published in the Proceedings of the Santa Cruz e^-e^- Workshop, Santa Cruz, CA, Sept. 4-5, 1995.
 34. J.F. Gunion and J. Kelly, Phys. Rev. **D51**, 2101 (1995); and in preparation.
 35. M.S. Chanowitz and M.K. Gaillard, Nucl. Phys. **B261**, 379 (1985).
 36. D. Burke, these proceedings.
 37. J. Bagger, V. Barger, K. Cheung, J.F. Gunion, T. Han, G.A. Ladinsky, R. Rosenfeld, and C.-P. Yuan, Phys. Rev. **D52**, 2878 (1995).
 38. V. Barger, K. Cheung, T. Han, and R.J.N. Phillips, Phys. Rev. **D52**, 3815 (1995).
 39. The constraints on a fourth generation in the context of supergravity models can be found in J.F. Gunion, D.W. McKay, and H. Pois, Phys. Rev. **D53**, 1616 (1996).
 40. For a recent survey, see V. Barger, M.S. Berger, and R.J.N. Phillips, Phys. Rev. **D52**, 1663 (1995).
 41. J.L. Hewett and T.G. Rizzo, Phys. Rep. **183**, 193 (1989).